UDC 629.5.015.4:629.5.035

Morteza GHASSABZADEH[1]
Hassan GHASSEMI[1]
Maryam Gh. SARYAZDI[2]

Determination of Hydrodynamics Characteristics of Marine Propeller Using Hydro-elastic Analysis

Professional paper

The paper presents a method based on hydro-elastic analysis to determine the hydrodynamics characteristics of a marine propeller using a hybrid BEM-FEM software code. In the method, the hydrodynamic load acted on the propeller is determined by a BEM code and the deformed propeller is then obtained by an FEM code in every step. The iterations between the BEM and FEM are repeated till the deflection and hydrodynamic characteristics (thrust, torque and efficiency) of the propeller are converged. The effects of skew angle on the performance of a composite propeller are also studied. As the skew angle increases, the maximum deflection of blade increases, however, thrust and torque coefficients decrease. Additionally, a copper high tensile brass propeller is analyzed and the results are compared to the composite one.

Keywords: *hydro-elastic analysis, marine propeller, propeller characteristics, skew angle*

Određivanje hidrodinamičkih značajki brodskog vijka korištenjem hidroelastične analize

Stručni rad

Ovaj rad daje prikaz metode temeljene na hidroelastičnoj analizi koja služi za određivanje hidrodinamičkih značajki brodskih vijaka korištenjem hibridnog BEM-FEM softverskoga koda. Hidrodinamička opterećenja na vijak određuju se putem BEM koda, te se deformacija vijka dobiva korištenjem FEM koda iterativnim putem. Iteracije između BEM i FEM ponavljaju se sve do konvergiranja vrijednosti otklona i hidrodinamičkih svojstava (poriv, moment i korisnost). Učinci kuta izvoja na značajke kompozitnog vijka također su proučavani. Kako raste kut izvoja maksimalni otklon krila raste, dok se poriv i moment smanjuju. Dodatno, mesingani vijak s bakrom visoke elastičnosti je analiziran, te su rezultati uspoređeni s kompozitnim vijkom.

Ključne riječi: *hidroelastična analiza, brodski vijak, značajke vijka, kut izvoja*

Authors' addresses (Adrese autora):
[1] *Department of Ocean Eng., AmirKabir University of Technology,* Tehran, Iran: e-mail: gasemi@aut.ac.ir
[2] *Vehicle Research Centre, AmirKabir University of Technology,* Tehran, Iran e-mail: mgharyazdi@aut.ac.ir

Received (Primljeno): 2011-07-27
Accepted (Prihvaćeno): 2012-06-11
Open for discussion (Otvoreno za raspravu): 2014-03-31

1 Introduction

Marine propeller is the most efficient element that operates behind the ship's stern to generate thrust, from the pressure load acting on the blade, to drive the marine vehicle. Because of the loading on the propeller, its reaction may be significant in the performance obtained from hydro-elastic analysis. The common materials from which propellers are made can be classified as bronzes, stainless steels, copper, aluminium and composite materials. Nowadays, the use of composite materials increases because they have the useful acoustic properties and a high strength to weight ratio. Because of the hydrodynamic and mechanical forces acting on the propeller, the shape of blades changes in real working conditions. Therefore, the propeller should be analyzed considering the interaction of the fluid and structures, namely hydro-elastic analysis. The study of the effect of deformations on the propeller performance may be an interesting topic for researchers to optimize the propeller design.

In primary researches, the forces are applied on the blade and their stress-strain reactions are calculated using analytical and experimental relations. The application of shell elements is presented for the prediction of quasi-static and dynamic stresses in marine propeller blades [1]. A coupled boundary element method (BEM) and finite element method (FEM) is applied for the numerical analysis of flexible composite propellers in the uniform flow and in the wake inflow [2]. The method is able to predict the hydrodynamic loads of blade and stress distributions and deflection patterns of flexible composite propellers. The effects of material and loading uncertainties on the delivered thrust, advance speed, cavitation inception boundary, and material failure boundary are determined using a validated 3-D BEM-FEM model [3]. Young & Savander performed numerical analysis of a large scale surface-piercing propeller [4]. A coupled structural and fluid flow analysis is carried out [5] to assess the hydro-elastic behaviour of a composite marine propeller. A MAU propeller is analyzed with different stacking sequences of composite layup. The hydro-elastic behaviours of the propeller with balanced and unbalanced stacking sequences are investigated and discussed [6]. A comprehensive work is carried out on the

hydro-elastic tailoring of the flexible composite propeller [7]. The stress distribution and the deflection of blades in the steady flow are computed by the thick shell finite element method in combination with the surface panel method [8]. Chau analyzed the marine propeller and compared the stress-strain field in 2-D and 3-D [9]. Note that the same problem may occur in the ship hull due to the impulsive loads of slamming that causes whipping. Malenica et al. presented the methodology for the hydro-elastic analysis of the ship hull [10].

The SPD (Ship Propeller Design) software code is prepared and employed to various propulsions such as propeller-rudder system (PRS) [11], high skewed propeller [12], contra-rotating propeller [13], and surface piercing propeller [14]. The SPD software is well-verified for the calculation of hydrodynamic performance of all types of immersed propellers; however, for the hydro-elastic calculations it should be more researched.

This paper presents a method in which the coupled BEM-FEM code is used for propeller hydro-elastic analysis. Note that the present BEM-FEM code is currently non-commercial software but it is validated by the experimental data. The deformed shape of the propeller may be determined by an iterative method. The hydrodynamic forces are calculated by modelling the fluid-structure interaction in a boundary element code. The deformation of the blades is then calculated using a finite element model. In the case study, the geometry of the deformed composite propeller is determined for four values of skew angles and the effect of deformations on the propeller performance is examined for several values of advanced coefficient. A copper high tensile brass propeller is also analyzed and compared to the composite one to examine the effect of material.

2 BEM-FEM code

2.1 BEM for hydrodynamic analysis

The boundary element method is based on Green's theory in which the governing equations of the volume domain are transferred to the boundary of the body [15]. Therefore, in three-dimensional problems, the surface elements may be used to analyze the model. In the BEM code, the boundary surface of the propeller is discretized into quadrilateral elements, as shown in Figure 1. The problem solution uses the combined potential flow and boundary layer theories. Since the propeller is a lifting body, the thrust and torque are defined on the basis of the pressure effect which is determined by potential flow using BEM. The frictional force is based on 2D boundary layer theory using ITTC empirical formulae.

Using the boundary element techniques and boundary layer theory, the hydrodynamic pressure (p_h) and tangential stress (τ) are determined as follows:

$$\begin{cases} p_h = 0.5\rho\left(2\vec{V}_R.\nabla\phi - \nabla\phi.\nabla\phi\right) \\ \tau = 0.5\rho.C_F.V_R^2 \end{cases} \quad (1)$$

The total thrust and torque of the propeller are determined as follows:

$$\begin{cases} T = \int_S p_h n_x ds + \int_S \tau n_x ds \\ Q = \int_S p_h\, r(n_y z - n_z y) ds - \int_S \tau\, r(n_y z - n_z y) ds \end{cases} \quad (2)$$

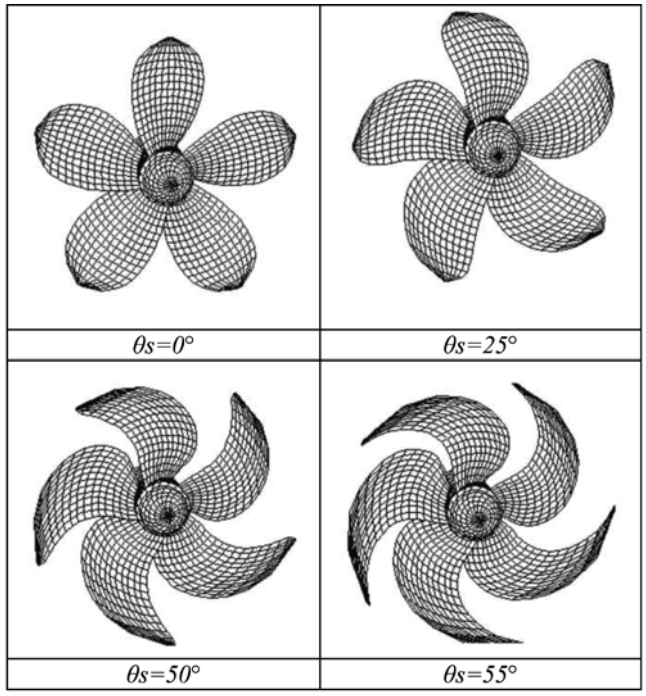

Figure 1 **Mesh surface of the undeformed propellers at four skew angles in the BEM**
Slika 1 **Mreža površine nedeformiranog vijka pri četiri kuta izvoja u BEM modelu**

Figure 2 **Comparison of the open water characteristics for the B4.40 propeller model**
Slika 2 **Usporedba karakteristika slobodne vožnje vijka za B4.40 model vijka**

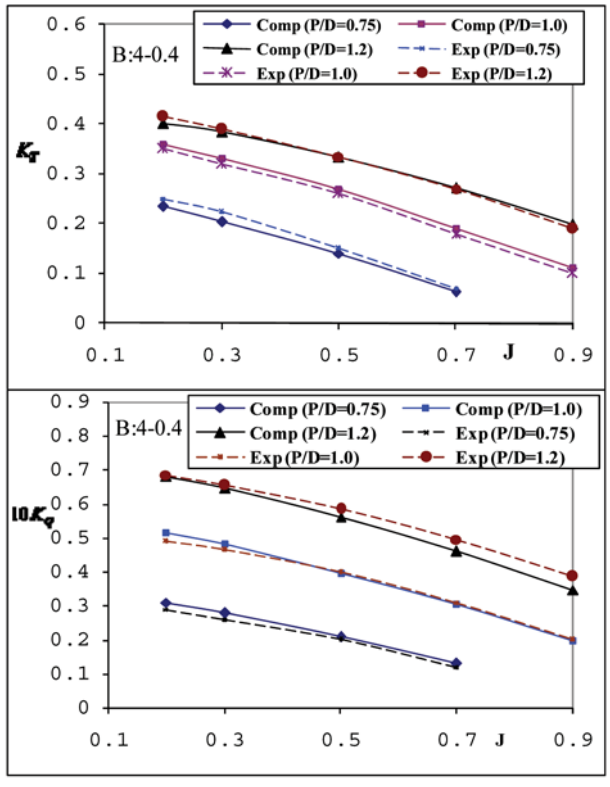

The hydrodynamic characteristics of the propeller (thrust and torque coefficients and efficiency) can be defined as follows:

$$K_T = \frac{T}{\rho n^2 D^4}, \qquad K_Q = \frac{Q}{\rho n^2 D^5}$$
$$\eta_o = \frac{J}{2\pi}\frac{K_T}{K_Q}, \qquad J = \frac{V_A}{nD} \tag{3}$$

For validation of the BEM code, K_T and K_Q obtained from the analysis of B-series of marine propeller with four blades and expanded area ratio of 0.4 are compared to experimental data. As shown in Figure 2, a good agreement exists between the BEM results and the experimental data.

2.2 FEM for structural analysis

The finite element code, in this paper, is used for the structural analysis of propeller. A macro is generated and imported to the FEM code in which the blade geometry is generated automatically using the general characteristics of the propeller and the boundary conditions and loads are applied. The FEM model of propeller is then analyzed and the results data are exported to the output file.

In the generated macro, the geometry model is meshed regularly with the three dimensional solid element with 20 nodes. The finite element model is created according to *x, y* and *z* coordinates of the nodes used in the BEM model. Therefore, the results of the FEM can be simply transferred to the BEM code.

In the global frame, the discrete equation of motion can be written as follows:

$$[M]\{\ddot{u}\} + [C]\{\dot{u}\} + [K]\{u\} = \{F_{ce}\} + \{F_P\} + \{F_g\} \tag{4}$$

where $[\ddot{u}]$, $[\dot{u}]$ and $[u]$ are acceleration, velocity and displacement, while $[M]$, $[C]$ and $[K]$ are structural mass, damping and stiffness matrices respectively. $\{F_{ce}\}$ is the centrifugal force vector calculated by the following equation:

$$F_{ce} = \int_v \rho_P r_e \omega^2 dv \tag{5}$$

where r_e is the radial position of the centre of the element, ρ_P is the density of the blade and ω is the rotational speed of propeller and dv is the volume, defined by multiplication of the thickness, $t(r)$, at each radius into dr, i.e. $dv=t(r)dr$. $\{W\}$ is the gravity force vector calculated for each element by the following equation:

$$W = \int_v \rho_P g dv \tag{6}$$

$\{F_h\}$ represents the sum of the hydrodynamics and the hydrostatics forces calculated for each element by the following equation:

$$F_h = \int_A p dS \tag{7}$$

p is the total pressure acted on each element. It is determined by

$$p = p_h + p_0 + \rho g\left(Y_{CE} + H\right) \tag{8}$$

where p_0 is the atmospheric pressure, H is the depth of the hub below the free surface and Y_{CE} is the position of the element centre in the Y direction. The hydrodynamic pressure p_h is calculated by the BEM code and imported to the FEM.

Note that the loading conditions of blades depend on their position. In every revolution, the maximum load is applied to each blade once. In the vertical and downward position, the critical load is applied to each blade. In this situation, the gravity and centrifugal forces are in the same direction. In addition, the summation of atmospheric pressure, hydrostatic pressure (due to head of water above the hub) and hydrodynamics pressure are applied on the surface blade.

3 Case study

In this study, a five-bladed propeller is selected to examine the effect of deformations on the propeller performance. The main dimensions of the propeller are given in Table 1. The maximum blade thickness ratio at $r=0.2R$ is the same for both materials. The analyses are executed for four skew angles of 0, 25°, 50° and 55°. The material properties of the composite [16] and the copper high tensile brass propeller are listed in Table 2. It is assumed that the composite propeller is made of linear elastic anisotropic composite laminates stacked in the thickness direction.

Table 1 **Main dimensions of the propeller**
Tablica 1 **Glavne dimenzije vijka**

Parameters	Values
Number of blades (Z)	5
Diameter (D)	0.75 (m)
Hub ratio (r_h/R)	0.2
Pitch ratio (P/D)	0.80
Expanded Area Ratio (EAR)	0.65
Max. thickness ratio (t_{max}/D)	0.045
Skew angle (θs)	Variable
Rake angle	10 (deg.)

Table 2 **Material properties of propeller**
Tablica 2 **Značajke materijala vijka**

Materials / Parameters	Composite	Copper high tensile brass
Modulus of elasticity (GPa)	E_x=132 E_y=10.8 E_z=10.8	E_z=102.97
Poison coef.	v_{xy}=0.24 v_{yz}=0.49 v_{xz}=0.24	v_{xz}= 0.35
Shear Modulus of elasticity (GPa)	G_{xy}=5.65 G_{yz}=3.38 G_{xz}=5.65	-
Density [ton/m^3]	ρ_p = 1.5	ρ_p = 8.25

In the analysis, for the sake of simplicity and time saving, one blade of the propeller is modelled. It is assumed that the root of blade is fixed. The forces acting on the blade are included in the hydrodynamics loads (thrust and torque), centrifugal and gravity forces. The maximum resultant force may happen when the blade is in vertical and downward position, because the centrifugal and gravity forces are in the same direction.

To achieve the grid independency of the model, several FEM models are created with different element size. The size of elements is reduced step wisely until the results are converged to the same one after a specific step. Figure 3 shows the finite element model of the blade. Because of the complicity of tip geometry and sudden reduction of blade section, the elements of blade tip are refined in this region.

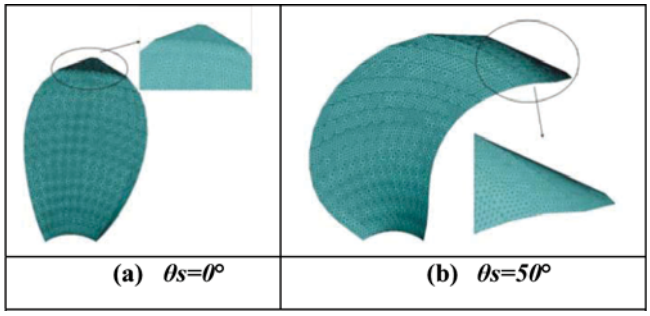

Figure 3 **Finite element model of the blade**
Slika 3 **Model krila vijka od konačnih elemenata**

First, a three-dimensional model of undeformed blade is analyzed in the BEM code to calculate the hydrodynamic pressure. The results are then exported to the FEM software to calculate the deformation of the blade. This procedure is repeated until the maximum deformation, efficiency, thrust coefficient and torque coefficient converge. The hydro-elastic analysis of each blade is done for eight amounts of advance velocity ratio: J=0.2 to 0.9 with step of 0.1. Note that the operating condition of the propeller is relatively heavy at $J=0.2$, so the stress and deflection are higher than in other conditions. For this reason, the most results are shown at this condition. Figure 4 shows the convergence of the parameters for the skew angle of 0^0 and 55° at J=0.2. The variations of the parameters vanish after 14 and 6 steps of hydro-elastic analysis of the composite propeller for the skew angle of 0^0 and 55°, respectively. However, this is 5 steps for the copper high tensile brass propeller at the skew angle of 55°.

Figure 4 **Convergence steps of K_T, K_Q and efficiency for skew angle of 55° of brass and composite blades and 0° of composite blade at $J=0.2$**
Slika 4 **Koraci konvergiranja K_T, K_Q i korisnosti za kut izvoja od 55° za mesingana i kompozitna krila te za 0° za kompozitna krila pri $J=0,2$**

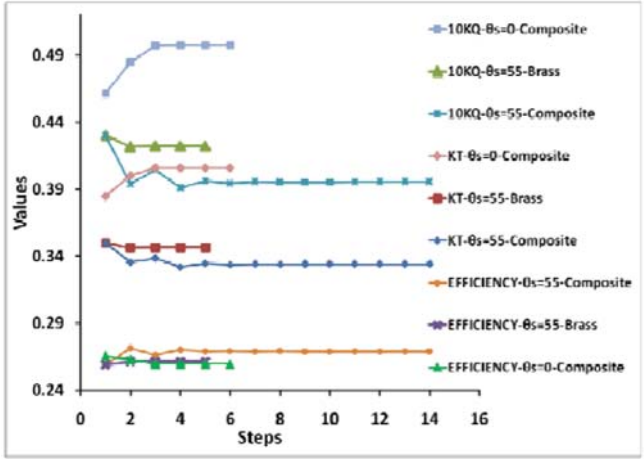

In each step of the analysis, the hydrodynamic pressure distribution changes due to deformation of the blade. Figure 5 shows the deflection of tip blade in the X direction at the consecutive steps of the hydro-elastic analysis for the skew angle of 50° at $J=0.2$. In the first step the X deflection is negative; however in the second step it will be positive. It is observed that the deflection fluctuates until the solution converges. The fluctuating and converging of the deflection from the 4th step to the 9th step is depicted in the lower figure. The convergence steps of the brass and composite propeller characteristics are shown in Figure 6. The solution for the brass propeller is converged with fewer steps than for the composite one.

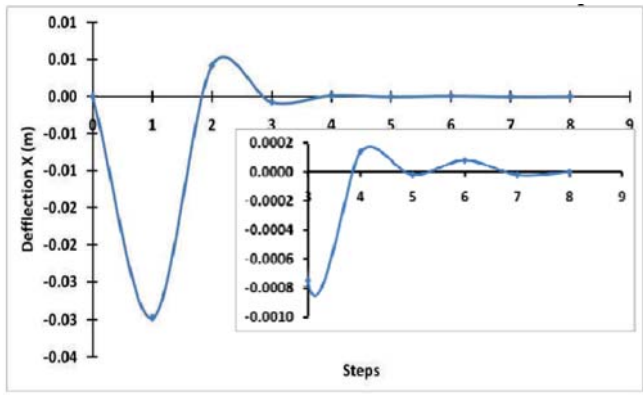

Figure 5 **Deflection of tip composite blade in X direction at the consecutive steps of hydro-elastic analysis (skew angle of 50° at $J=0.2$)**
Slika 5 **Pomaci vrha kompozitnog krila u smjeru X pri uzastopnim koracima hidroelastične analize (kut izvoja od 50° pri $J=0,2$)**

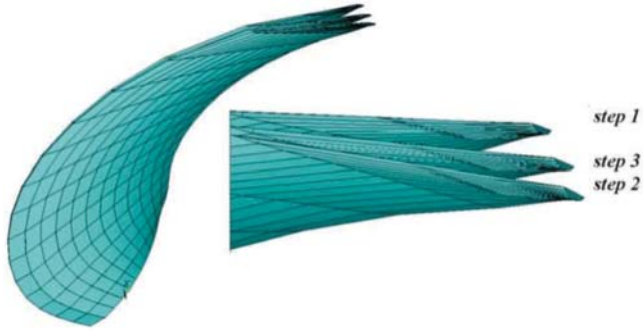

Figure 6 **Deformation of composite blade at three first steps of hydro-elastic analysis (skew angle of 50° at $J=0.2$)**
Slika 6 **Deformacija kompozitnog krila pri tri prva koraka hidroelastične analize (kut izvoja od 50° pri $J=0,2$)**

Figure 7 shows the stress versus the skew angle for the composite blade at $J=0.2$. In the figure, σ_1 is the maximum principal stress, σ_x is the normal stress in the x direction and τ_{yz} is the shear stress. σ_1 and σ_x will be maximum at $\theta_s=25°$. However, τ_{yz} increases as the skew angle increases. The maximum deflection of the blade versus the advanced velocity ratio is shown in Figure 8 for both the composite and the brass blade. The deflection of the composite blade at $\theta_s=50°$ is much greater than that of the

copper high tensile brass blade especially at a lower loading condition (i.e. at lower J).

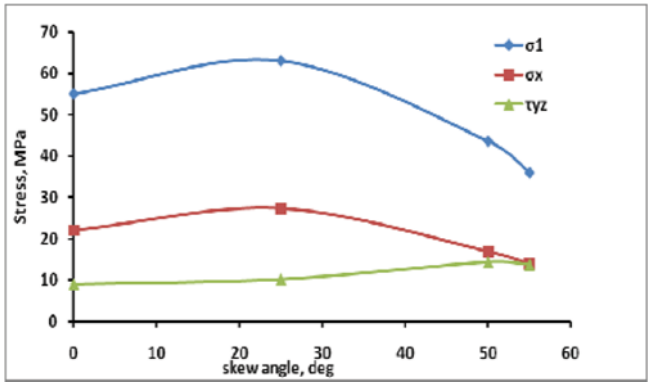

Figure 7 **Stress versus the skew angle for the composite blade at *J=0.2*.**
(σ_1: maximum principal stress, σ_x: normal stress in x direction and τ_{yz}: shear stress)
Slika 7 **Naprezanje u odnosu na kut izvoja za kompozitno krilo pri *J=0,2***
(σ_1: maksimalno osnovno naprezanje, σ_x: normalno naprezanje u smjeru x i τ_{yz}: smično naprezanje)

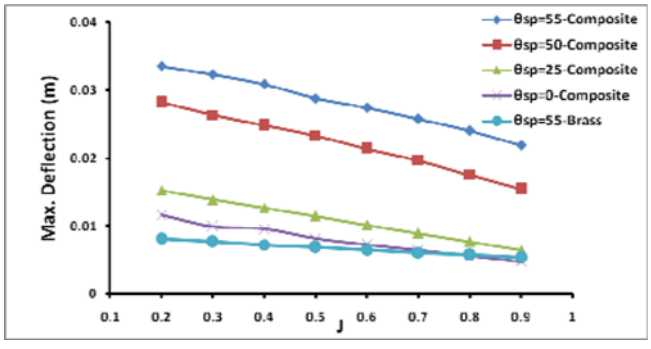

Figure 8 **Maximum deflection of the blade versus the advanced velocity ratio**
Slika 8 **Maksimalan otklon krila u odnosu na omjer napredovanja**

Figure 9 **Hydrodynamic characteristics for undeformed and deformed composite blades (θ_s=0)**
Slika 9 **Hidrodinamičke značajke za nedeformirano i deformirano kompozitno krilo (θ_s=0)**

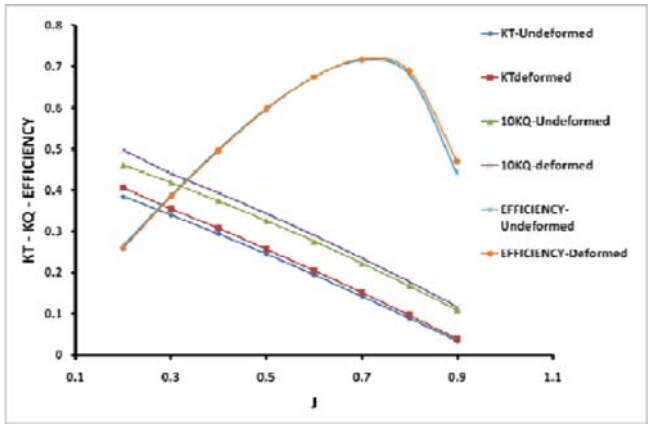

The hydrodynamic characteristics of the deformed and undeformed shape of the composite propeller (K_T, K_Q and efficiency) for θ_s=0 are shown in Figure 9. The efficiency of the deformed blade is nearly equal to that of the undeformed one up to J=0.7. However, the coefficients of K_T, K_Q of the deformed blade are higher than those of the undeformed one.

The hydrodynamic characteristics of the deformed and undeformed shape of the composite and the brass propeller for θ_s=55° are shown in Figure 10. The efficiency of the deformed blade is higher than that of the undeformed one for J<0.6, however for J>0.6 it is opposite. The coefficients of K_T, K_Q of the deformed blade are lower than those of the undeformed one. The hydrodynamic characteristics of the deformed brass blade are nearly equal to those of the undeformed one.

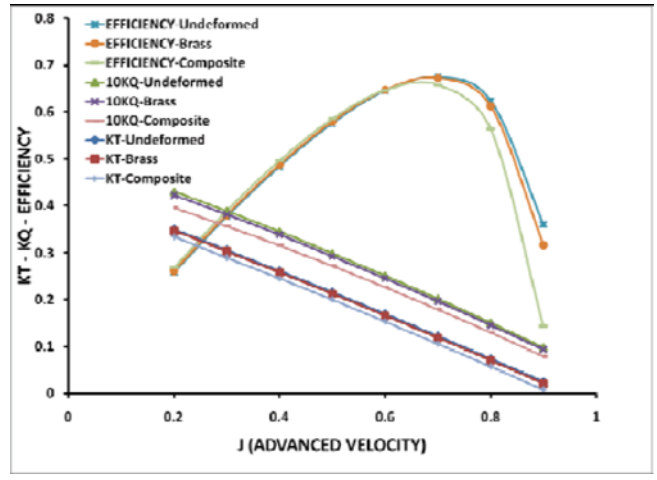

Figure 10 **Hydrodynamic characteristics for undeformed and deformed blades of brass and composite materials (θ_s=55°)**
Slika 10 **Hidrodinamičke značajke za nedeformirana i deformirana krila od mesinga i kompozitnog materijala (θ_s=55°)**

4 Conclusion

In this paper, a flexible marine propeller is analyzed using the hydro-elastic BEM-FEM code in which the coupling hydrodynamic and structural analyses are considered. The prepared code implements an iteration approach to predict the deformed shape of the propeller. The hydrodynamics force is calculated by modelling interaction of solid-fluid in the BEM code. The deformation of the propeller is then determined using a finite element software.

In the case study, a propeller with five blades is chosen to study the effect of deformation on the propeller performances. The composite propeller is analyzed for four values of skew angles at the advanced velocity ratios of 0.2 to 0.9 and the copper high tensile brass propeller is analyzed at the skew angle of 55°. The maximum value of efficiency occurs at more advanced velocity ratios as the skew angle increases. The efficiency of the deformed blade is higher than that of the undeformed one up to an amount of J at which the efficiency will be maximum, and for higher values of J it is opposite. The deformation of the brass propeller is less than that of the composite one, so the hydrodynamic

characteristics of the deformed brass blade are nearly similar to those of the undeformed one.

List of symbols

C_F :	friction coefficient [-]
D :	diameter of propeller [m]
E :	modulus of elasticity [Pa]
EAR:	expanded area ratio [-]
F_{ce}:	centrifugal force [N]
F_h :	hydrodynamic force [N]
g:	gravity acceleration [m/s^2]
G:	shear modulus of elasticity [Pa]
H:	the water depth of the hub [m]
J:	advance velocity ratio [-]
K_Q:	torque coefficient [-]
K_T:	thrust coefficient [-]
n:	propeller rotation speed [RPS]
n_x, n_y, n_z:	unit normal vector in x, y, z direction [-]
r:	radius of the propeller section [m]
r_h/R:	hub ratio [-]
r_e:	radial position of element centre [m]
T:	thrust of propeller [N]
t_{mzx}/D:	maximum thickness ratio [-]
P/D:	pitch ratio [-]
p_0:	atmospheric pressure [Pa]
p_h:	hydrodynamic pressure [Pa]
Q:	torque of propeller [Nm]
$\vec{V}_R$:	resultant inflow velocity [m/s]
$\vec{V}_A$:	advance velocity [m/s]
$[M]$, $[C]$, $[K]$:	mass, dumping, and stiffness matrices [kg, Ns/m, N/m]
$[\ddot{u}]$, $[\dot{u}]$, $[u]$:	acceleration, velocity, and displacement [m/s^2, m/s, m]
W:	gravity force [N]
Y_{CE}:	position of the element centre in the Y direction [m]
Z:	number of blade [-]
ρ:	water mass density [kg/m^3]
ρ_p:	propeller mass density [kg/m^3]
ν:	kinematic viscosity [m^2/s]
ν_{xy}, ν_{xy}, ν_{xy}:	Poison coefficient [-]
ω (=$2\pi n$):	rotational velocity [rad/s]
σ_1:	maximum principal stress [Pa]
σ_x:	normal stress in x direction [Pa]
τ_{yz}:	shear stress [Pa]
τ:	tangential stress [Pa]
$\nabla\phi$:	derivative of velocity potential [m/s]
θ_s:	skew angle [deg.]
η_o:	propeller efficiency [-]

References

[1] SONTVEDT, T.: "Propeller blade stress application of finite element methods, Computers & Structures, 4 (1974), p.193-204.

[2] YOUNG, Y.L.: "Hydro-elastic behaviour of the flexible composite propeller in wake inflow", 16th Conf. on Composite Materials, Kyoto, Japan, 2007.

[3] YOUNG, Y.L.: "Fluid–structure interaction analysis of flexible composite marine propellers", Journal of Fluids and Structures, 24(2008), p.799–818.

[4] YOUNG, Y.L., SAVANDER, B.R.: "Numerical analysis of large-scale surface-piercing propellers", Ocean Eng., 38(2011), 13, p.1368-1381.

[5] BLASQUES, J.P., BERGGREEN C., POUL ANDERSEN, P.: "Hydro-elastic analysis and optimization of a composite marine propeller", Marine Structures, 23(2010).

[6] LIN H.J., LAI W.M., KUO, Y.M.: "Effect of stacking sequence on nonlinear hydro-elastic behaviour of composite propeller", Journal of Mechanics, 26(2010)3.

[7] MULCAHY, N.L., PRUSTY, B.G., GARDINER C.P.: "Hydro-elastic tailoring of flexible composite propellers", Ships and Offshore Structures, 5(2010)4, p.359–370.

[8] GEORGIEV D.J., IKEHATA, M.: "Hydro-elastic effects on propeller blades in steady flow", Journal of the Society of Naval Architects of Japan, 184 (1998), p.1-14.

[9] CHAU, T.B.: "2-D Versus 3-D Stress analysis of a marine propeller blade", Zeszyty Naukowe Akedemii Morskiej W. Gdyni, nr 64, lipiec 2010.

[10] SENJANOVIĆ, I., MALENICA, Š., TOMAŠEVIĆ, S., RUDAN, S.: "Methodology of Ship Hydroelasticity Investigation", Brodogradnja (Shipbuilding), 58(2007)2, p.133-145.

[11] GHASSEMI, H., GHADIMI, P.: "Computational hydrodynamic analysis of the propeller-rudder and the AZIPOD systems", Ocean Engineering, 34(2007), p.117-130.

[12] GHASSEMI, H.: "The effect of wake flow and skew angle on the ship propeller performance", Scientia Iranica, 16(2009)2, p.149-158.

[13] GHASSEMI, H.: "Hydrodynamic performance of coaxial contra-rotating propeller (CCRP) for large ships", Polish Maritime Research, 16(2009)1, p.22-28.

[14] GHASSEMI, H.: "Hydrodynamic characteristics of the surface-piercing propellers for the planing craft", Journal Marine Science Application, 7(2008), p.147-156.

[15] KATSIKADELIS, J.T.: "Boundary Elements, Theory and Applications", Elsevier Science publication Ltd, 2002.

[16] ROBERTO, O., B. GANGADHARA, P., G., MARCOS, S.: "Finite element investigation on the static response of a composite catamaran under slamming loads", Ocean Engineering, 31 (2004), p. 901–929.